Conformal Array Beam Synthesis and Taper Efficiency Comparisons

Paul G. Elliot, Lead Engineer. MITRE Corp.
202 Burlington Road, Bedford, MA, 01730-1420 USA
email: pelliot@mitre.org

ABSTRACT
In order to increase antenna placement options on crowded platforms, three methods for synthesizing conformal phased array excitations on curved surfaces were computer programmed and compared: the Alternating Projections method (AP), the Successive Projections method (SP), and the Genetic Algorithm method (GA). The comparison was based on how closely the synthesized patterns conformed to the desired pattern amplitudes, and on the resulting taper efficiency. An expression for taper efficiency of a curved array was derived, showing directivity compared to a linear array. Greater efficiency would increase gain for a given antenna size. Taper efficiency is useful in evaluating the synthesis methods since different methods can produce very different aperture illuminations despite similarity in the resulting patterns. Curved arrays were computer modeled ranging from 17 to 97 elements. Different initial excitations, element patterns, and desired pattern masks were investigated. The AP method synthesized patterns closest to the desired patterns, closely followed by the GA method. The SP method tended to get stuck in local minima for difficult cases. The GA method was programmed to optimize taper efficiency, but it takes much longer to run than the other two methods.

KEY WORDS: phased-array antennas, conformal array synthesis, beam scanning capability, taper efficiency.

1. Introduction and Problem Formulation

This paper addresses efficient beamforming techniques for conformal phased array antennas. The far field radiation pattern $Fr(\theta,\phi)$ of a general array is given as:

$$Fr(\theta,\phi) = \sum_{n=1}^{N} a_n g_n(\theta,\phi)\, e^{+j\frac{2\pi}{\lambda}(x_n u + y_n v + z_n c)} \qquad (1)$$

where:

a_n is the nth element's complex excitation (amplitude and phase).

$g_n(\theta, \phi)$ is the complex element directivity pattern of the nth element in the array environment, with its far-field phase referenced to the element's local origin at x_n, y_n, z_n.

N is the number of elements

x_n, y_n, z_n = location of nth element

λ = wavelength

u = $\sin\theta \cos\theta$

v = $\sin\theta \sin\theta$

c = $\cos\theta$

Equation (1) allows the elements to have arbitrary locations so the array can be curved. For the ith far field direction (θ_i, ϕ_i), Eq. (1) can be written as:

$$Fr_i = \sum_{n}^{N} G_{i,n} a_n \qquad (2)$$

Where

$$G_{i,n} = g_n(\theta_i, \phi_i) e^{+j\frac{2\pi}{\lambda}(x_n u_i + y_n v_i + z_n c_i)} \qquad (3)$$

$G_{i,n}$ is therefore the complex element directivity pattern of the nth element in the ith far-field direction, with its far-field phase reference now translated to the array common origin. Eq. (2) can be written in matrix form as:

[Fr] = [G][A] (4)

where the column vector **[A]** contains all the complex excitations a_n for the array elements, and **[Fr]** is a column vector with the far field values at the set of far field points i, and **[G]** is a complex matrix with i as the row number and n the column number. Therefore each individual pattern point is computed using one row of **[Fr]** and **[G]** and using the entire column vector **[A]**. The **[G]** are also known as the "basis functions" in Eq. (4). The system of equations in Eq. (4) is typically overdetermined (has more rows than columns, requiring more field points than number of elements). If element patterns are measured or computed in the array environment with other elements terminated, then the a_n are incident forward voltages at each element.

2. Synthesis Methods Programmed

Using Eq. (4) we applied three conformal array synthesis methods to obtain a desired far field directivity pattern **[Fd]**, without concern for the phase of the pattern which is usually of much less interest than amplitude. The three methods programmed were: the Alternating Projections (AP) method, the Successive Projections (SP) method, and the Genetic Algorithm (GA) method. All three methods are iterative and are described in the references. The comparison between synthesis methods was based on how closely the synthesized patterns conformed to the desired pattern amplitudes, and also on the resulting taper

efficiency. MATLAB was used for the computer programming. Other synthesis methods were briefly reviewed using published literature, several are summarized in [1]. The three methods programmed were selected for some of the following reasons: widely used (AP, GA), fast convergence (AP, SP), resistant to local minima (GA), easily incorporate additional optimization criteria (GA), not limited to larger radii of curvature (all 3), availability of information describing the method (all 3), and pre-programmed software tools (GA).

The Alternate Projections (AP) Method [2,3,4,5,6] is fast and yielded patterns that most closely met the desired pattern masks in our study. The steps for AP synthesis are summarized as follows (details are in the references):

(a) Use an initial or preceding array excitation to compute **[Fr]** in Eq.4. (b) Determine an **[Fd]** by making minimum amplitude adjustments in **[Fr]**. (c) Solve system of equations **[G][A] = [Fd]** using least-squares for a new **[A]** that minimizes the difference **[G][A] - [Fd]**. (d) Repeat from step (a).

The Successive Projections (SP) Method [7] is also fast but we found the SP method tended to get stuck in local minima for difficult cases. The projection we used for this method is given by [7]:

$$\left[\mathrm{A}^{\mathbf{k}}\right]=\left[\mathbf{A}\right]+\left\{\frac{\mathrm{F}_{\mathrm{d}}^{\mathrm{k}}}{\mathrm{F}_{\mathrm{r}}^{\mathrm{k}}}-1\right\}\frac{\mathrm{F}_{\mathrm{r}}^{\mathrm{k}}}{\mathbf{G}^{\mathbf{k}}\cdot\mathbf{G}^{\mathbf{k}*}}\mathbf{G}^{\mathbf{k}*} \qquad (5)$$

Where

[A] is the previous excitation vector for all elements

[A^k] is the new excitation vector, it will yield zero pattern error at the i=k pattern point.

k is value of i indicating the pattern point with the largest error between desired and realized patterns

G^k is one row of matrix $G_{i,n}$ of basis functions defined in Eq. (3) (with i=k and including all elements n).

G^{k*} is the Hermetian conjugate of G^k (i.e. complex conjugate of each term of G^k

For the Genetic Algorithm (GA) method we used MATLAB's easy-to-use Genetic Algorithm Toolbox [8]. For GA, a 'population' or set of many different excitation vectors **[A]** is improved by mimicking biological evolution. Each real or imaginary part of each element excitation of **[A]** was considered a "gene", so if there are N elements in the array, there were 2N genes in each excitation vector **[A]**, and we usually set the population size equal to 2N also. The GA applies a fitness test to each **[A]** based on how closely the realized pattern **[Fr]** fit a desired pattern **[Fd**] at each pattern point, and the highest scoring **[A]** used to generate the next generation. The fitness cost function we used for GA was:

$$\text{Score}= \left(\sum(\,|\,\mathbf{[G][A]}\,|\,-\,|\,\mathbf{[Fd]}\,|\,)^2\right)^{1/2} + W_e\,\varepsilon_{T\,db} \qquad (6)$$

Where the pattern difference summation is done over all the pattern points, $\varepsilon_{T\,db}$ is the taper efficiency in dB, and W_e is the weight selected for taper efficiency.

Eq. (6) is similar to the least squares metric usually used in the AP method, but in Eq. (6) the absolute values of the fields are used since **[G][A]** is complex but it is only the far-field amplitude we really need to synthesize. Also the taper efficiency is optimized when W_e is non-zero.

For this study the baseline GA parameters included a population size that was double the number of elements and the synthesis was run for 5000 generations. This was apparently sufficient since increasing the number of generations rarely produced any significant improvement for these problems. However, if population was decreased and generations increased proportionally, those two changes approximately canceled each other so it usually produced equivalent results and run-times as the GA baseline.

The GA provides a robust global 'random walk' convergence. As shown in Eq. 6, the GA easily added additional optimization goals such as taper efficiency, but this produces a tradeoff between the different optimization goals, generally neither goal is met as fully as would be possible if it was the only goal. The results depend in large part on how heavily each goal is weighted relative to the other goal(s).

3. Array Geometries

Several different curved arrays were modeled, two are reported on here and are summarized in Table 1. For each array, a single curved column of elements was modeled. Both curves are portions of a circle: the small arc subtends 120°, and the large semi-circle subtends 180°. The element spacing along each curve was 0.5 wavelengths. The far-field pattern cuts were synthesized in the plane containing the curve. The small arc (sa) is almost identical to the array used by reference [4].

Table 1. Curved Array Geometries

Array Curve Shape (and abbreviation)	# Elem	Array Width (Chord Length)
Small Arc (sa)	17	7 wavelengths
Large Semi-Circle (ls)	97	32 wavelengths

4. Directivity Masks

All three synthesis methods use a desired directivity mask to synthesize a far field pattern that lies within the upper and lower bounds of the mask. Two masks are reported on in this paper:

4.1 Cosecant-squared Pattern Mask (CSC):

This is a $\csc^2$ power pattern from +5° to +35°, with -20 dB max sidelobes from -180° to 0°, and -30 dB max

sidelobes from +40° to +180°. It is listed in Table 2a. 0-5° and 35-40° are the skirts of the main lobe. The peak of the beam is near +5°, and the half-power beamwidth is approximately 10° wide. This mask was the easier of the two to synthesize since the wide beamwidth is realizable using a small array. This mask is very similar to a mask used in another paper [4].

Table 2a. Desired Directivity Mask "CSC"

Angles	Desired Level
-180° to -90°	< -30 dB
-90° to 0°	< -20 dB
+5° to +35°	$\csc^2$ ±1 dB
+40° to +180°	< -30 dB

4.2 Pencil-beam and Notch Pattern Mask (P3N):
This is a pencil-beam scanned to -69°, and with a -55 dB notch from -5° to +5°, and -30 dB max sidelobes at other pattern angles. It is listed in Table 2b. The -30 dB beamwidth is therefore 9°. To meet this mask completely requires the use of the larger array (ls).

Table 2b. Desired Directivity Mask "P3N"

Angles	Desired Level
-180° to -74°	< -30 dB
-69°	0 ±1 dB
-65° to -5°	< -30 dB
-5° to +5°	< -55 dB
+5° to +180°	< -30 dB

5. Element Patterns

An ideal planar array with element spacing ≤ λ/2 has a cosine element power pattern ($\cos^q$ with q=1) due to the projected area in the direction of the main beam, assuming perfect match at every scan angle. However, for this study a cosine-squared element power pattern was used since q=2 agrees better with measured patch element patterns on a curved wing array seen in the figures of reference [3] where q ranged from q=1.3 to q=2.9. It was found that a narrow element pattern improved the synthesis results. The element pattern peak value was 1 and was in the direction normal to the array curve at the element location. Mutual coupling is not included except via the approximation of the element pattern.

6. Initial Array Excitations

Three different initial array excitations were tried and are listed in Table 3. The AP and SP methods started with one initial excitation: either UAUP or UACP. For UACP the array initially has phase coherence in the desired main beam direction. UACP was found to give higher efficiency and/or lower sidelobes than a broadside initial collimation or UAUP. For the GA method both UAUP and UACP were included in the initial populations along with numerous random initial illuminations. The initial amplitudes used for all cases are close to the anticipated average amplitude after synthesis, which was found to yield patterns closer to the mask than starting with initial amplitudes that are much larger or smaller.

Table 3. Initial Array Excitations

Initial Array Excitation	Abbreviation	Methods
Uniform Amplitude Uniform Phase	UAUP	AP, SP
Uniform Amplitude Collimated Phase	UACP	AP, SP
Both of the above	BOTH	GA

7. Taper Efficiency

Taper efficiency is used to indicate how efficiently the physical length of the antenna is utilized and how much directivity can be expected from the array taper compared to a broadside linear array. Taper Efficiency for linear arrays is defined as [9,10,11,12]:

$$\varepsilon_T = \frac{1}{N} \frac{\left|\Sigma a'_n\right|^2}{\Sigma\left|a'_n\right|^2} \qquad (7)$$

Where N is the number of elements and a'_n is the n^{th} element's complex excitation for a broadside beam [10,12]). Eq. (7) is "a measure of coherence for a linear array. The numerator is proportional to the total coherent field, squared, whereas the denominator is proportional to the sums of the squares of the individual fields from the various elements" [12]. The directivity D_0 of a broadside linear array is related to the above taper efficiency by $D_o = N\varepsilon_T$ which is exact only for a linear array of isotropic elements spaced λ/2 apart. For a planar array the analogous quantity is called aperture efficiency.

For curved arrays Eq. (7) needs to be modified. Firstly, because in the curved array, the numerator of Eq. (7) is not collimated for broadside beam by simply using equal phases, so a broadside collimating phase shift based on element locations needs to be included so that the numerator is again proportional to the peak power of the beam at broadside. Secondly, Eq. (7) uses isotropic element patterns which gives equal weight to all elements, which could give quite misleading taper efficiency values because in a curved array the element patterns face in different (sometimes even opposite) directions, unlike a large linear array where most of the element patterns are the same in any given direction. For a curved array some of the elements may not radiate at all in the desired main beam direction. As a result, using isotropic elements to compute taper efficiency for a curved array can easily produce a meaningless value for realistic elements which do not have the same element pattern in the main beam direction. Therefore the following formula for Taper Efficiency was used for curved arrays:

$$\varepsilon_T = \frac{1}{N} \frac{\left| \sum_n^N a_n G_{ip,n} \right|^2}{g_{\max} \sum_n^N |a_n|^2} \qquad (8)$$

$G_{ip,n}$ is the complex element directivity pattern of the nth element in the ipth far-field direction, with phase referenced to the array common origin, as defined earlier in Eq. (3). The subscript ip denotes the direction (θ_{ip}, ϕ_{ip}) which is the direction of the desired peak of the array main beam. g_{max} is the maximum magnitude of the element directivity pattern. For the computations in this report g_{max} = 1 since the element field pattern is cosine.

Eq. (8) yields a taper efficiency between 0 and 1 equal to the ratio of the curved array directivity to the directivity of a uniform broadside linear array with the same number of elements and element pattern. Eq. (8) is therefore analogous to Eq. (7) modified for a curved array and including the element pattern. Taper efficiency computed using Eq. (8) was also used as an optimization goal for some GA cases as shown in Eq. (6), in which case the efficiency weight W_e is non-zero and shown under the plot title. If W_e is not shown on the plot then W_e was zero.

Using the GA an attempt was also made to improve taper efficiency by minimizing the total power radiated as part of the optimization cost function (instead of using Eq. 8), but this approach did not provide improved taper efficiency.

8. Results

The patterns show far-field relative directivity in dB. The θ=0 angle bisects the arc of the arrays so it can be considered as broadside. The plot titles use abbreviations shown earlier, and the taper efficiency is also shown. If the taper efficiency was optimized (GA method only) then W_e from Eq. (6) is also shown in the plot title. The AP will reproduce identical results when re-running the same geometry and initial excitation. This is also true of SP, but not the GA due to random initial excitations and mutations.

8.1 Cosecant-Squared (CSC) Pattern Mask Results:

All three synthesis methods and all the array geometries were able to synthesize the CSC mask. Figure 1 shows some patterns for the smallest of the arrays with the CSC mask overlay. The GA pattern in Fig. 1 has been optimized for efficiency as well as pattern which produced a significant improvement in efficiency with a small cost to the pattern since it is seen that the ½ dB improvement in efficiency comes at a cost of not quite making the desired pattern mask at a couple of points in the main beam region. If the efficiency is weighted too heavily as in Figure 2, then it causes the main beam to narrow too much. In general for small arrays, the AP and GA methods met the CSC mask more closely and with higher efficiency than the SP.

Figure 1. 17-Element Small Arc (sa) Array Patterns, Using AP and GA Methods.

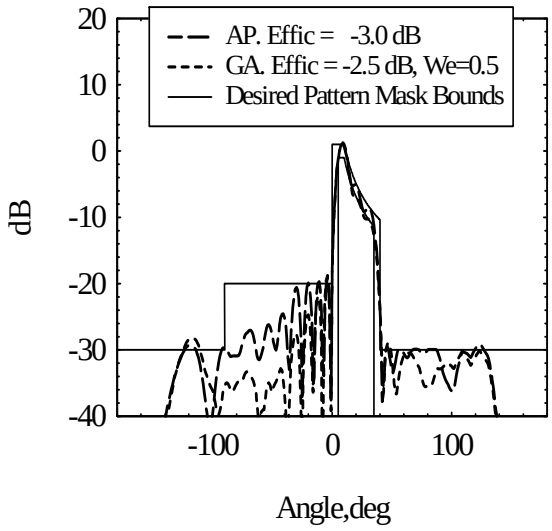

Figure 2. 17-Element Small Arc (sa) Array Pattern, GA Method, CSC Mask, Taper Effic = -1.7 dB, We = 2.0

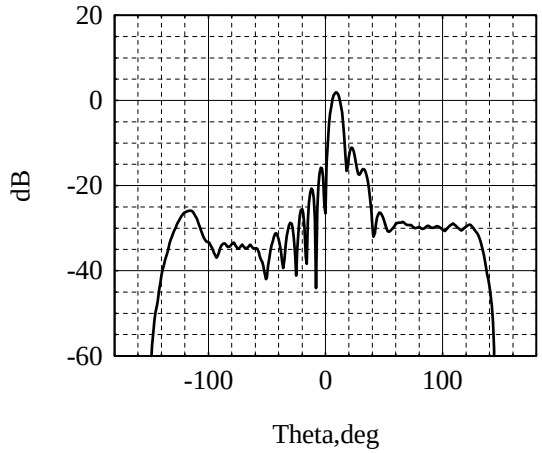

For the large array (ls), all three synthesis methods produced CSC patterns that closely conformed to the mask. Fig. 3 shows a sample result using SP. The SP produced the highest (i.e. best) taper efficiencies and the AP the lowest taper efficiencies, and the UACP initial illumination resulted in higher efficiency than UAUP. Optimizing for efficiency at just the beam peak as shown in Fig. 4 does not help for the larger array with a wide beamwidth because it pushes up a narrow peak within the broad-beam of the mask. It therefore might have worked better to optimize efficiency over a wide range of angles by integrating taper efficiency in Eq. (8) over the entire main beam region, not just optimizing the efficiency in one beam direction. This may help with Fig. 2 also. This was not tried yet due to time limitations.

Fig. 3. 97-Element Large Semi-Circular (ls) Array
SP Method, UAUP, CSC Mask. Taper effic = -10.7 dB

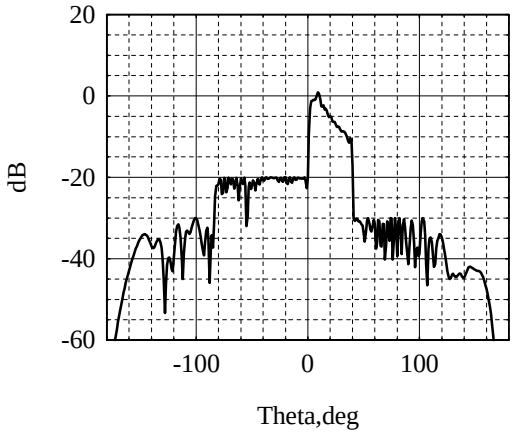

Figure 4. 97-Element Large Semicircular (ls) Array Pattern,
GA Method, CSC Mask, Taper Effic = -4.5 dB, We = 0.5

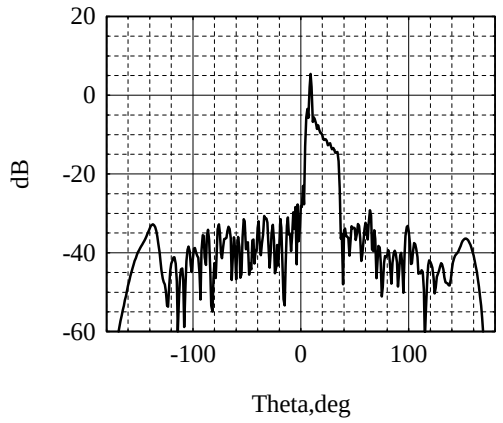

8.2 Scanned Pencil Beam with Notch (P3N) Results

Using the largest array (ls) all three synthesis methods met the P3N mask. Figure 5 shows an example using the AP method, the only shortfall for all the methods was that the notch is only 8 degrees wide instead of 10 degrees. Also with the SP UAUP the notch was not quite -55 dB deep at some points. The UACP again gave higher efficiency than UAUP, and the SP gave slightly higher efficiencies than AP, with GA intermediate in efficiency. The GA results showed significant variations in notch depth from one run to the next due to random excitations. Optimizing the GA for efficiency improved efficiency at a a cost to the pattern notch and sidelobes as seen in Fig. 6. Several smaller arrays of varying sizes were also tried but the aperture size projected in the main beam direction was not wide enough to fully meet the P3N mask requirements, the results deteriorating as the array size is reduced. The AP method came closest to meeting the mask. The GA came the second closest. It was noted in numerous cases that the SP did not degrade as gracefully and gave especially poor patterns for these more difficult masks, apparently getting stuck in local minima. Here, UACP typically resulted in a pattern closer to the mask than UAUP.

Figure 5. 97-Element Large Semicircular (ls) Array Pattern,
AP Method, UACP, P3N Mask, Taper Effic = -5.1 dB

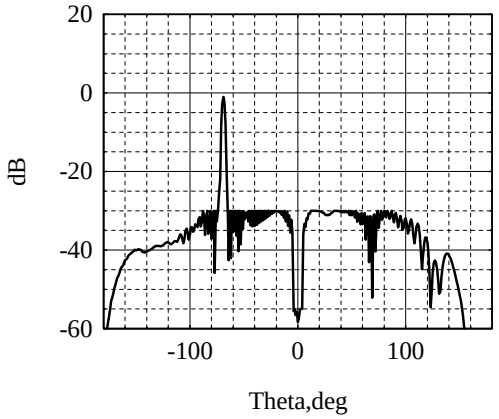

Figure 6. 97-Element Large Semicircular (ls) Array Pattern,
GA Method, P3N Mask, Taper Effic = -4.4 dB We = 0.5

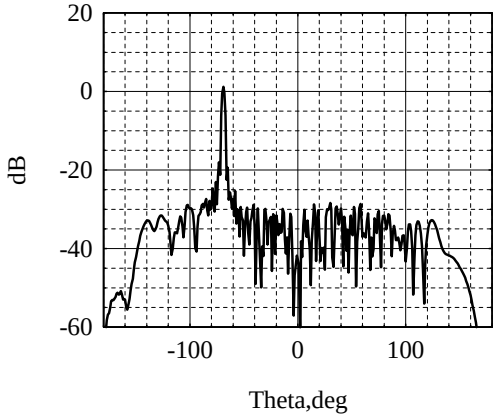

Figure 7 shows the effect of a wider element pattern: $\cos^q$ with q=1 element power pattern was used instead of q=2 which was selected for all the other cases as explained in Section 5. A comparison of Figs. 5 and 7 shows the patterns deviate much more from the desired mask when using the wider element pattern (q=1). This was also noted for several other cases. This is probably because the spatial selectivity offered by the narrower element field of view (q=2) allows each pattern point to be synthesized using a smaller number of elements, with each pattern point less affected by elements in other parts of the array, i.e. each far field point is coupled to fewer elements, which makes optimization easier. A narrower element pattern also reduces back-radiation.

8.3 Excitation Taper Results

It was noted that the smaller arrays with the highest (i.e. best) taper efficiency also visually showed the smoothest amplitude taper. However, this could not be discerned visually for the larger arrays or for the phase excitations. It was also found that different synthesis methods can

produce very different aperture illuminations despite the similarity in the resulting patterns.

Figure 7. 97-Element Large Semicircular (ls) Array Pattern, Using Wider Element Pattern (q = 1)
AP Method, UACP, P3N Mask, Taper Effic = -2.8 dB

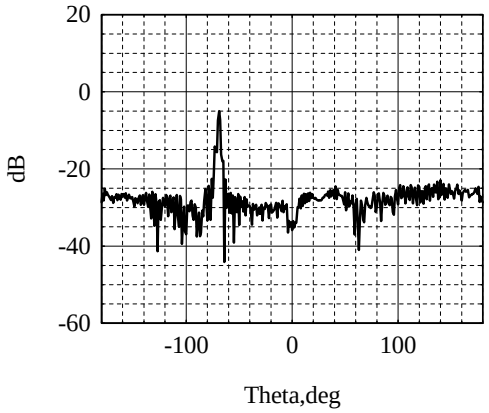

8.4 Run Times

Run time in MATLAB on a PC for the AP and SP methods was typically 5 to 45 seconds for the largest array (ls) to converge, depending on the difficulty of the mask. The number of iterations required was from 10 to 500. AP usually required fewer iterations but each iteration of SP was faster. The GA was much slower: 14 hours for the ls array for the baseline GA. The GA is too slow for real-time beam-shaping but could be used for preset beams using look-up tables. The taper efficiency optimization added negligible time.

9. Conclusions

The synthesis methods programmed can be used as versatile tools to synthesize array excitations for array geometries. Of the three methods, the AP most often produced a pattern that met or almost met the desired pattern mask; the GA was almost but not quite as effective as AP in this regard. The SP method met the mask for the easier cases, but for difficult pattern requirements the SP tended to converge to a pattern that deviated much more from the desired mask, apparently getting stuck in a local minimum. In terms of speed the AP and SP were both approximately equally fast, and the GA needed a very much longer run-time.

Different synthesis methods can produce very different aperture illuminations despite the similarity in the resulting patterns, and some of these illumination functions may be more useable or higher efficiency than others. An expression for taper efficiency of a curved array was derived. Taper efficiency indicates how efficiently the physical area of the antenna is utilized and how much directivity can be expected compared to a linear array. The GA method was programmed to optimize taper efficiency which could often produce gains in efficiency. A narrow element pattern produces synthesized patterns that more closely meet the mask than a wider element pattern. An initial excitation that was collimated and scanned to the desired direction often resulted in higher efficiency and lower sidelobes than starting with uniform phases. Results were also better using initial excitations near the same order of magnitude as the resulting element amplitudes.

10. Acknowledgement

This work was supported by Air Force Contract FA8721-04-C-0001: “Enabling Technologies for Mobile Communications”.

References

[1] R. F. E. Guy, R. A. Lewis, and P. J. Tittensor, “Conformal Phased Arrays,” First European Workshop on Conformal Antennas, 1999, pp. 4-7.

[2] H. Steyskal, “Pattern Synthesis for a Conformal Wing Array,” *IEEE Aerospace Conference*, Big Sky, MT, pp. 2-819 – 2-824, March 2002.

[3] D. Curtis, B. Tomasic, R. Thomas, S. Santarelli, and H. Steyskal, “Measurement and Analysis of a Conformal Wing Array,” *Antenna Applications Symposium*, Allerton Park, Monticello, IL, pp. 192-220, Oct. 2001. (Has a good summary of AP method on pg. 203).

[4] L. Josefsson and P. Persson, “Conformal Array Synthesis Including Mutual Coupling,” *Electronics Letters*, vol. 35, no. 8, pp. 625-627, 15 April 1999.

[5] O. M. Bucci and G. D’Elia, “Power Synthesis of Reconfigurable Conformal Arrays with Phase-Only Control,” *IEE Proc.-Microwave Antenna Propagation*, vol. 145, no. 1, pp. 131-136, Feb. 1998.

[6] G. Mazzarella and G. Panariello, “Pattern Synthesis of Conformal Arrays,” *1993 IEEE Antennas & Propagat. Society International Symposium*, pp. 1054-1057.

[7] G. T. Poulton, “Power Pattern Synthesis Using the Method of Successive Projections,” *IEEE Antennas & Propagation Society International Symposium*, pp. 667-670, 1986.

[8] *Genetic Algorithm and Direct Search Toolbox*, *User’s Guide*, Version 1. (for use with MATLAB). The MathWorks, Natick, MA, 2004.

[9] R. J. Mailloux, *Phased Array Antenna Handbook.* Boston: Artech house, 1994, p.26 and pp.70-71.

[10] R.C. Johnson and H. Jasik, *Antenna Engineering Handbook.* NY: McGraw-Hill, 1984, ch.20, p.15.

[11] R. S. Elliott, “The Theory of Antenna Arrays,” in *Microwave Scanning Antennas*, vol. 2, ch. 1, R. C. Hansen, Ed. New York: Academic Press, 1966, vol. 2, pg. 29.

[12] R. S. Elliott, *Antenna Theory and Design.* Englewood Cliffs, NJ: Prentice-Hall, 1981. pg. 154.